# Reversible Stolt migration

William A. Burnett[*] and Robert J. Ferguson

## ABSTRACT

The nonstationary equivalent of the Fourier shift results in a general one-dimensional integral transform that applies to many seismic data processing steps. This general transform is, computationally, a simple matrix-vector multiplication, and it is a tool for implementation. Here, this general transform is used to implement a reversible Stolt migration.

## INTRODUCTION

Although quite complex in development, frequency-wavenumber (*f-k*) migration is mechanically performed by a simple one-dimensional, nonstationary shift in the *f-k* domain. Many methods exist to perform migration other than *f-k*. The advantages and disadvantages of each relative to each other will be left out here, and no attempt is made here to discuss when *f-k* migration is appropriate for creating a final image. Many authors have such discussions (i.e., (Yilmaz, 2001)), and although not critical to the development here, they may provide some insight into appropriate uses of transforms in processing flows.

Frequency wavenumber migration was developed by Stolt (1978). Today, *f-k* migration is still regarded as the most efficient migration method for simple velocity models. The major limitation of *f-k* migration is that it does not handle laterally varying velocity models. Because of this, it is today rarely used to create final seismic images in industry. However, in cases where diffractors or multiples can be isolated by migrating with a simple velocity model, *f-k* migration by data processing transform is practical.

The theory of *f-k* migration is built upon some of the very basic principles of reflection seismology combined with a single subtle feature of the 2-D Fourier transform. As shown below, a primary goal of any migration method is to increase the dips of unmigrated events. The amount that each dip is increased depends on the migration velocity and the original dip. The 2-D Fourier transform moves time-space (*t-x*) data to the frequency-wavenumber domain, where all events with the same dip (regardless of location in the input image) map to a radial line from the *f-k* origin.

Then, essentially a “frequency moveout” correction is applied, very similar in form to the NMO correction, which moves events to appropriately steeper dips. Hyperbolic curves in the *t-x* domain collapse and the data are now migrated.

It is useful to discuss exactly how dipping events are affected by migration. This is done by observing the geometry of reflection events with respect to the geometry of their associated reflectors. Figure 1 shows how a dipping event on a zero offset section relates to the correct, migrated position of its reflector. The shift moves events from their apparent

[*]University of Texas, Austin

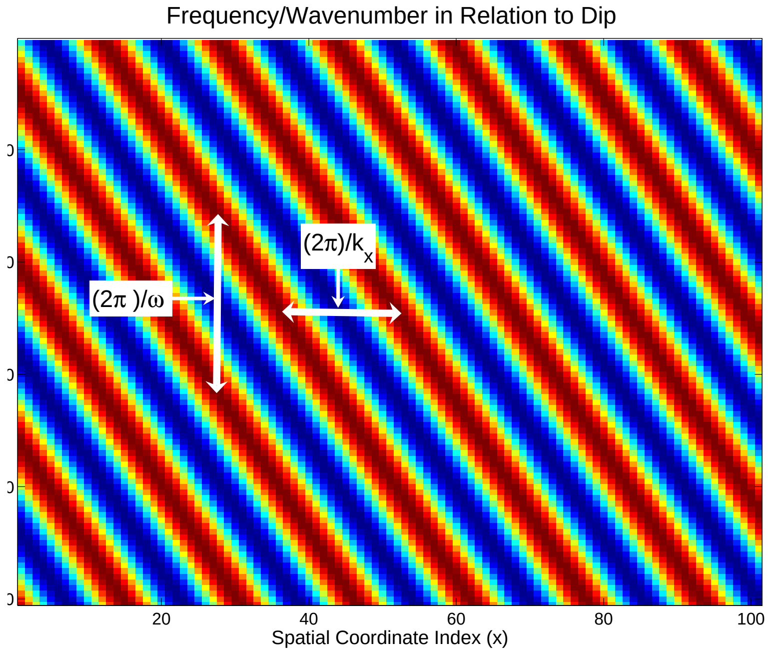


FIG. 1. A single plane wave in the *t-x* domain. Notice here how the ratio of the wavenumber ($k_x$) to the frequency ($\omega$) is the same as the dip of the events. In this case, the dip is 2 time samples per 1 space sample.

dip, $\theta_a$, to the migrated dip, $\theta_m$ by (Stolt, 1978)

$$\theta_m = \sin^{-1}\left(\tan\left(\theta_a\right)\right). \tag{1}$$

The flanks of hyperbolae have changing dip, and this expression also collapses each hyperbola in an image to its apex. The fact that equation 1 collapses hyperbolae is the first hint that if migration can be done by *shifting* the dips of events, then it may be a nonstationary shift.

Next, it is important to establish why the *f-k* domain allows events recorded at their apparent dips to shift to their appropriate migrated dips. The single 2-D plane wave image in Figure 1 shows how the ratio of frequency to wavenumber defines the dip of an event in the image. Assuming any seismic image is the superposition of plane waves, (Yilmaz, 2001), all events with the same frequency to wavenumber ratio will then have the same dip in the *t-x* domain, and they will plot along a radial line in the *f-k* domain.

Next, a relation between the apparent and migrated dips in the *f-k* domain is needed. Derived from the Fourier transform of the two-way wave equation, (Yilmaz, 2001), the dispersion relation provides it:

$$\omega = \frac{v}{2}\sqrt{k_x^2 + k_z^2}. \tag{2}$$

Instead of the apparent and migrated dips as in equation 1, this expression conveniently and equivalently relates their frequency to wavenumber ratios. For a constant wavenumber in those ratios, $\omega$ corresponds to the recorded apparent dip, and $k_z$ corresponds to the migrated dip.

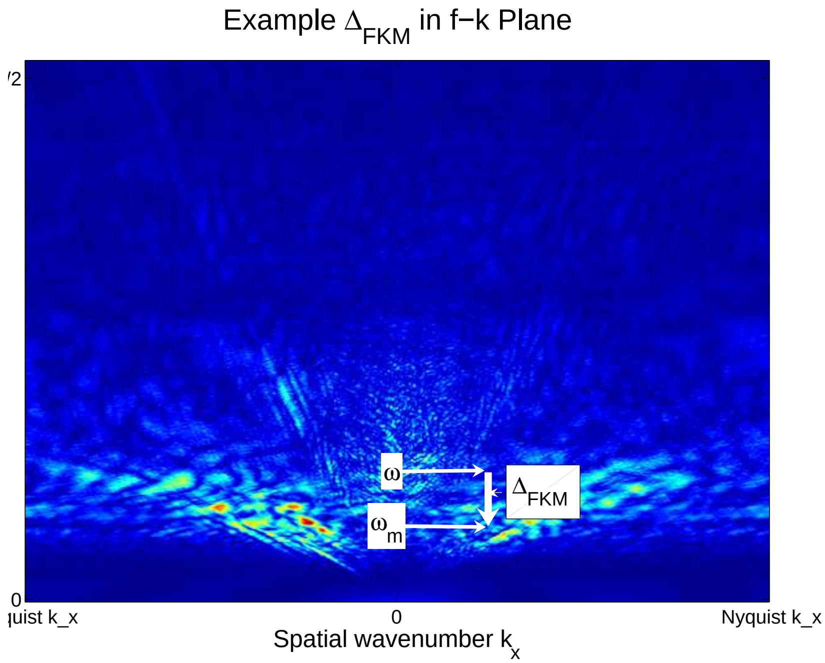


FIG. 2. Example shift for *f-k* migration. After combining the dispersion relation with geometric features of the 2-D Fourier transform, migration can be performed in the *f-k* domain with a 1-D nonstationary shift. The shift amount, $\Delta_{FKM}$, changes with wavenumber and is nonstationary because of its dependence on $\omega$ and $\omega_m$.

Equation 2 is the instrument for migration in the frequency wavenumber domain. The dispersion relation is strikingly similar to the NMO equation, and indeed has the same mechanical meaning. This time, instead of moving data from $t_x$ to $t_0$, the goal is to move data from $\omega$ to $k_z$. Since $k_z$ is defined in the dispersion relation as the Fourier dual of the depth coordinate, $z$, shifting data from $\omega$ to $k_z$ corresponds to depth migration. This particular type of *f-k* migration is called Stolt migration ((Yilmaz, 2001), (Stolt, 1978)). Stolt migration is a 1-D nonstationary shift along the frequency axis in the *f-k* domain. Conventional Stolt migration algorithms rely on interpolation in the *f-k* domain, just as conventional NMO algorithms rely on interpolation in the *t-x* domain. The following section describes how to cast Stolt migration as a transform using the general form of the data processing transform of Burnett (2008b).

## THEORY

introducing a new variable, $\omega_m$, into equation 2 gives a relation between the input frequency and an output frequency that is related to the vertical wavenumber, proportional to velocity, (Karl, 1989).

$$\omega = \sqrt{\frac{v^2 k_x^2}{4} + \omega_m^2}. \tag{3}$$

In the *f-k* domain, migration is simply performed for each wavenumber by shifting data from its unmigrated frequency, $\omega$ to its migrated frequency $\omega_m$. This is just a 1-D nonstationary shift, so from the general data processing transform, the migration transform is quickly derived.

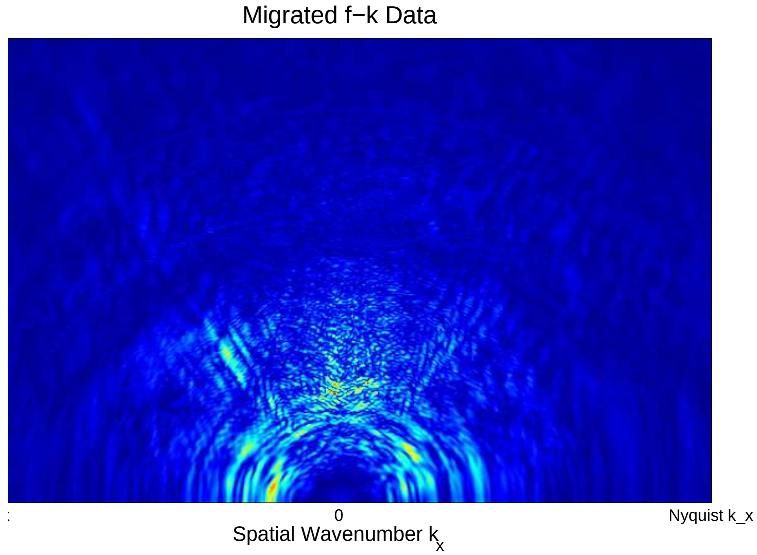


FIG. 3. Migrated *f-k* section. The same dataset as in Figure 2 after migration with a velocity of 1000 m/s. Notice how the radial lines in the unmigrated data have been mapped to arcs in this set. A 2-D inverse Fourier transform of this data yields the migrated data in the *t-x* plane.

Only two values are needed for each *f-k* point, $\Delta_{FKM}$, and $\alpha_{FKM}$. Identifying $\omega$ as the input coordinate and $\omega_m$ as the output coordinate for substitution into (Burnett, 2008b)

$$\Delta_{\mathrm{NMO}}\left(t_0\right) = t_x\left(t_0\right) - t_0. \tag{4}$$

and

$$\alpha = \frac{\partial p}{\partial q}. \tag{5}$$

(Burnett, 2008b) gives,

$$\Delta_{FKM} = \omega - \omega_m, \tag{6}$$

and

$$\alpha_{\mathrm{FKM}} \equiv \frac{\partial \omega}{\partial \omega_m} = \frac{\omega_m}{\omega} = \frac{1}{\sqrt{1 + \frac{v^2 k_x^2}{4\omega_m^2}}}. \tag{7}$$

These terms agree with conventional derivations of Stolt migration ((Stolt, 1978), (Karl, 1989)). But now the scaling factor commonly seen in *f-k* migration algorithms is explained and predicted simply by $\alpha_{FKM}$. The forward and inverse *f-k* migration transforms follow:

$$h\left(\omega_m\right) = \frac{1}{2\pi}\int_{-\infty}^{\infty} F(\beta) e^{\mathrm{i}\beta\omega(\omega_m)} d\beta, \tag{8}$$

and

$$F(\beta) = \int_{-\infty}^{\infty} \alpha_{\mathrm{FKM}} h\left(\omega_m\right) e^{-\mathrm{i}\beta\omega(\omega_m)} d\omega_m. \tag{9}$$

## IMPLEMENTATION

Implementation of Stolt migration using equations 8 and 9 is done with the same matrix-vector multiplication algorithm as described for the general case as in (Burnett, 2008b), and for NMO as in (Burnett, 2008a). The only major difference this time is that the input image is in the *f-k* domain to begin with. A regular 2-D FFT can be used to move an input gather into the *f-k* domain, where it is then treated as an image. The forward migration transform requires the 1-D (along the $\omega$ axis) Fourier transform of the *f-k* data as input. The transform then shifts the data back to the *f-k* domain while simultaneously performing the inverse Fourier transform. Since the Fourier transform can be defined with different sign and scaling conventions, (Sneddon, 1995), this means that the migration transform effectively maps between the unmigrated data cast in the *t-k* domain and the migrated data cast in the *f-k* domain. In equations 8 and 9, $\beta$ is left in as the Fourier dual of the input variable, in this case, it has the general definition of being the Fourier dual of $\omega$. Although it is effectively time, we choose to leave it unspecified, so that no change in Fourier transform convention is required in the middle of the data processing transform application. This same method of *f-k* migration by nonstationary filtering can be reduced to its specific and more concise form which shows that $\beta$ is indeed equivalent to the original *t-x* input time, *t*, (Margrave, 2001).

For this general transform approach, the matrices for the forward and inverse migration transform will have axes corresponding to discrete $\omega$ and $\beta$ values. The input signal vector will be the data at a single discrete wavenumber, $k_x$, and the output vector will correspond to an effectively moveout-corrected version of the data at that wavenumber. The matrix vector multiplication forms of equations 8 and 9 are given here:

$$h\left(\left(\omega_m\right)_j\right) = \sum_{l=1}^{N} a_{\mathrm{jl}} F\left(\beta_l\right), \tag{10}$$

and

$$F\left(\beta_j\right) = \sum_{l=1}^{N} b_{\mathrm{jl}} h\left(\left(\omega_m\right)_l\right), \tag{11}$$

where,

$$a_{\mathrm{jl}} = e^{\mathrm{i}\beta_l \omega\left(\left(\omega_m\right)_j\right)}, \tag{12}$$

and

$$b_{\mathrm{jl}} = \alpha_l e^{\mathrm{i}\beta_j \omega\left(\left(\omega_m\right)_l\right)}, \tag{13}$$

with no summation over *l* in 13. Examples of the migration transform matrices for a single wavenumber are given in Figures 4 and 5.

A normal 2-D inverse FFT recovers the migrated data from the result of equation 10. A standard 1-D inverse FFT along the $\omega$-axis followed by a regular 2-D inverse FFT recovers the original input data from the result of equation 11.

## DISCUSSION

Just as the NMO transform does in the *t-x* domain, the migration transform uses a Fourier basis to accurately interpolate the *f-k* image and apply a moveout correction. This

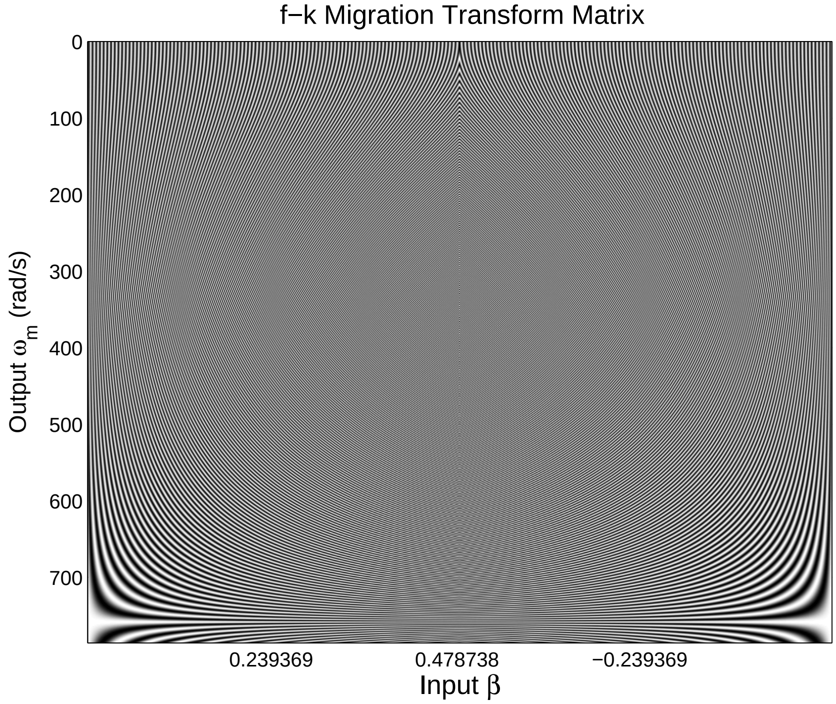


FIG. 4. The real part of an *f-k* migration transform matrix. The migration velocity was 1000 m/s, with time sampling and trace spacing at 4ms and 20m, respectively.

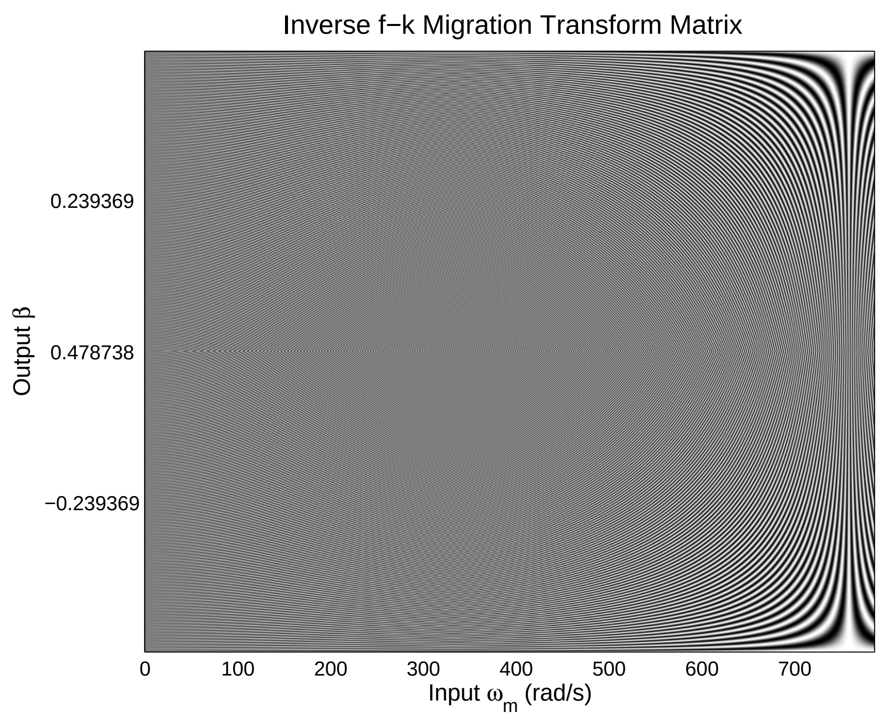


FIG. 5. The real part of an inverse *f-k* migration transform matrix. This matrix is the inverse of the matrix shown in Figure 4 within computational accuracy.

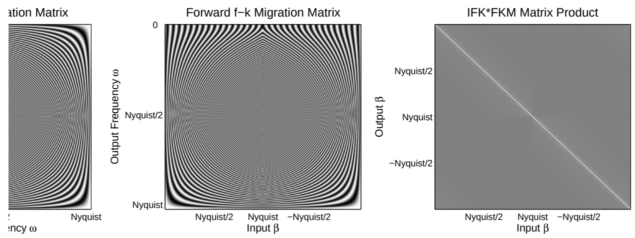


FIG. 6. The product of the inverse and forward migration matrices yields nearly the identity matrix. Only the real part of each matrix is shown.

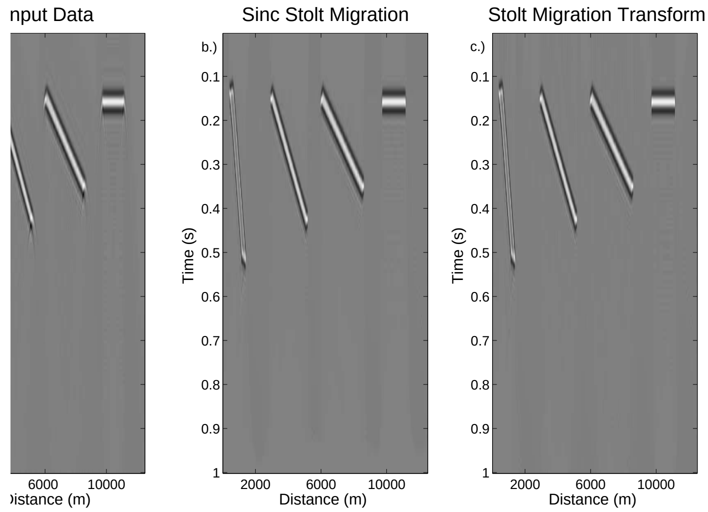


FIG. 7. Conventional migration (b.) and the *f-k* migration transform (c.) applied to a synthetic dataset (a.). The migration velocity is 1250 m/s, half of the velocity used to generate the synthetic input data. In the migrated sections, hyperbole are collapsed, dipping events are slightly steepened, and flat events are unaffected.

approach is quantitatively compatible with the Fourier transform, unlike conventional interpolation methods. Once again, this allows migration performed by the data processing transform to be exactly reversible in theory, and nearly reversible in practice.

Figure 6 shows how the product of the forward and inverse migration operator matrices is nearly the identity matrix. Second, we demonstrate that applying and removing *f-k* migration by transform recovers the input dataset very well in Figures 7, 8, and 9. Although not compared there to a conventional flow, the results would be very similar to the results of the conventional NMO application and removal flow. In conventional Stolt and *f-k* migration algorithms, interpolation is used to approximate frequency spectrum values between samples in the same way that interpolation is used in NMO to find intermediate time series values which results in data loss.

## ACKNOWLEDGEMENTS

The Jackson School of Geosciences, University of Texas at Austin, the EDGER Forum, and the sponsors of CREWES for supporting this research.

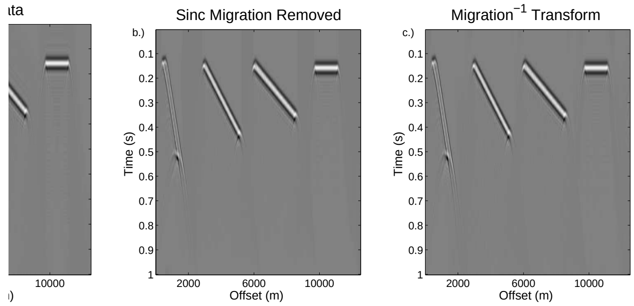


FIG. 8. Migration removed from panels b. and c. of Figure 7 using conventional inverse migration and the inverse migration transform, respectively. The data is recovered by the transform within computational accuracy. The difference sections for the two methods are shown in Figure 9.

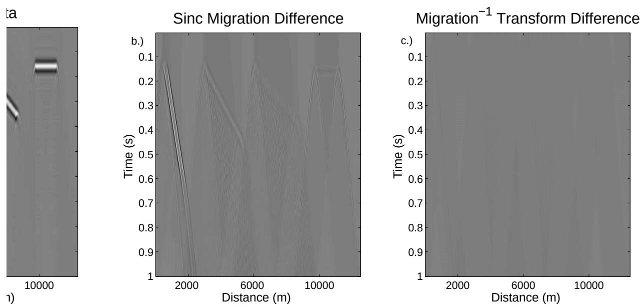


FIG. 9. Difference sections for conventional migration and the migration transform. Panels b. and c. show the difference between the input data and panels b. and c. in Figure 8, respectively. Unlike the conventional method, almost no data is lost during the forward and inverse migration transform. All three panels are to the same scale.

## REFERENCES

Burnett, W. A., 2008a, Reversible nmo: CREWES Research Report, **20**, 1–13.

Burnett, W. A., 2008b, A reversible transform for seismic data processing: CREWES Research Report, **20**, 1–17.

Karl, J. H., 1989, An Introduction to Digital Signal Processing: Academic Press.

Margrave, G. F., 2001, Direct fourier migration for vertical velocity variations: Geophysics, **66**, 1504–1514.

Sneddon, I. N., 1995, Fourier Transforms: Dover Publications.

Stolt, R. H., 1978, Migration by fourier transform: Geophysics, **43**, 23–48.

Yilmaz, O., 2001, Seismic Data Analysis: Society of Exploration Geophysics.